mathematics

MDPI

Article

A Novel Meshfree Approach with a Radial Polynomial for Solving Nonhomogeneous Partial Differential Equations

Cheng-Yu Ku [1,2], Jing-En Xiao [1,*] and Chih-Yu Liu [1]

1 Department of Harbor and River Engineering, National Taiwan Ocean University, Keelung 20224, Taiwan; chkst26@mail.ntou.edu.tw (C.-Y.K.); 20452003@email.ntou.edu.tw (C.-Y.L.)
2 Center of Excellence for Ocean Engineering, National Taiwan Ocean University, Keelung 20224, Taiwan
* Correspondence: 20452002@email.ntou.edu.tw; Tel.: +886-2-2462-2192 (ext. 6159)

Received: 27 January 2020; Accepted: 14 February 2020; Published: 18 February 2020

Abstract: In this article, a novel radial–based meshfree approach for solving nonhomogeneous partial differential equations is proposed. Stemming from the radial basis function collocation method, the novel meshfree approach is formulated by incorporating the radial polynomial as the basis function. The solution of the nonhomogeneous partial differential equation is therefore approximated by the discretization of the governing equation using the radial polynomial basis function. To avoid the singularity, the minimum order of the radial polynomial basis function must be greater than two for the second order partial differential equations. Since the radial polynomial basis function is a non–singular series function, accurate numerical solutions may be obtained by increasing the terms of the radial polynomial. In addition, the shape parameter in the radial basis function collocation method is no longer required in the proposed method. Several numerical implementations, including homogeneous and nonhomogeneous Laplace and modified Helmholtz equations, are conducted. The results illustrate that the proposed approach may obtain highly accurate solutions with the use of higher order radial polynomial terms. Finally, compared with the radial basis function collocation method, the proposed approach may produce more accurate solutions than the other.

Keywords: radial polynomial; radial basis function; collocation method; meshfree; nonhomogeneous

1. Introduction

The meshfree approach has attracted considerable attention, because through it, tedious mesh–generation can be avoided, and it has better computationally efficiency than other mesh-based methods [1–3]. The meshfree approach can be categorized into boundary-type and domain-type meshless methods depending on the basis function satisfying the governing equation or not [4]. Several domain–type meshless methods [5–7] have been proposed, such as the element-free Galerkin method [8,9], the meshless local Petrov-Galerkin method [10,11], the radial basis function collocation method (RBFCM) [12,13], the moving least squares approximation [14,15] and the generalized finite difference method [16–18].

In the RBFCM, the selection of the radial basis function (RBF) is of importance. The well-known RBFs are the Gaussian [19], multiquadric (MQ) [20] and thin-plate spline (TPS) functions [21–23], which can also be used to obtain the solution of the partial differential equation (PDE). For example, in 2008, Bouhamidi and Jbilou [24] applied the meshless radial basis function method based on TPS for solving modified Helmholtz equations. Among them, the MQ function may obtain more accurate results than other RBFs [25]. The MQ RBF is therefore often adopted as the interpolation function for solving PDEs. The RBFCM using the MQ function has been successfully applied in many physical, mathematical and engineering problems [26–28]. In 2017, Li and Hon [29] applied the finite integration method with RBF for solving stiff problems. The numerical results were compared with other spectral methods. Later, Liu and Chang [30] utilized the RBFCM to solve the Cauchy problems. In the RBFCM, it is necessary to determine the shape parameter. However, the issue for determining the proper value of the shape parameter in the MQ function still remains.

Since it has been a challenge to identify suitable values for the shape parameter of the MQ function, several attempts regarding this issue have been widely studied [31–33]. In 2010, Roque and Ferreira [34] used the leave-one-out cross-validation optimization technique for finding the ideal shape parameter to solve the boundary value problem. Afiatdoust and Esmaeilbeigi [35] applied the RBFCM in conjunction with the genetic algorithm to estimate the shape parameter for the solution of the ordinary differential equations. Biazar and Hosami [36] proposed a practical approach to determine the shape parameter within an interval instead of a value of the problem. The numerical results were then compared with those from other approaches. Recently, Chen et al. [37] proposed the RBFCM with the MQ RBF using the sample solution approach to determine the shape parameter for solving homogeneous and nonhomogeneous modified Helmholtz problems. Fallah et al. [38] adopted the MQ RBF for the seepage analysis in confined and unconfined porous media. The optimal shape parameter was chosen using a newly developed algorithm. It is worth mentioning that several innovative studies have been done using the polynomial basis function for the PDEs [39,40]. In 2017, Dangal et al. [41] adopted the polynomial particular solutions with the multiple scale technique for the simulation of the elliptic PDEs. Several numerical examples were conducted and compared with those from other approaches. Later, Lin et al. [42] presented an improved polynomial expansion method for solving plate bending vibration problems. In order to alleviate the conditioning of the matrix, the multiple-scale method was also employed. Besides, the TPS function can also be used to solve the PDEs [43], where the governing equation is discretized using the TPS on the collocation points within the domain. The singularity of the TPS may arise from the discretization of the governing equation. Xiang et al. [44] proposed to eliminate the singularity by adding an infinitesimal to the zero distance. Besides, the order of the TPS may also affect the accuracy of the solution, and it has to be chosen properly to obtain good convergence [45].

In this study, a novel, radial-based meshfree approach for solving nonhomogeneous PDEs is proposed. Stemming from the RBFCM, the novel meshfree approach is formulated by incorporating the radial polynomial as the basis function. The solution of the nonhomogeneous PDE is therefore approximated by the discretization of the governing equation using the radial polynomial basis function (RPBF). To avoid the singularity, the minimum order of the RPBF must be greater than two for the second-order PDEs. Since the RPBF is non-singular, accurate numerical solutions may be obtained by increasing the terms of the radial polynomial. In addition, the shape parameter in the RBFCM is no longer required in the proposed method. Several numerical implementations, including homogeneous and nonhomogeneous Laplace and modified Helmholtz equations, are conducted. The structure of this article is organized as follows. In Section 2, we present the formulation of the meshfree approach with a radial polynomial. Section 3 is devoted to giving several numerical examples. In Section 4, the discussion of this article is presented. Finally, conclusions are summarized in Section 5.

2. Formulation of the Meshfree Approach with a Radial Polynomial

We consider a domain bounded by the physical boundary, $\partial\Omega$, in two dimensions. The two–dimensional nonhomogeneous PDE can be written as follows

$$Du(\mathbf{x}) = f(\mathbf{x}) \text{ in } \Omega, \tag{1}$$

$$u(\mathbf{x}) = g(\mathbf{x}) \text{ on } \partial\Omega, \tag{2}$$

in which D represents a differential operator, $\mathbf{x} = (x, y)$; u is the unknown, which depends on the considered physical problem; Ω represents physical domain; $\partial\Omega$ denotes domain boundary; $f(\mathbf{x})$

and $g(\mathbf{x})$ represent the function values. Equation (1) is the Poisson equation if $D = \Delta$. On the other hand, it becomes the nonhomogeneous modified Helmholtz equation if $D = \Delta - \lambda^2$. A RBF is linearly independent, and can be generated using the one-dimensional Euclidean distance variable. The RBFCM is applied by assuming the following equation.

$$u(\mathbf{x}) = \sum_{j=1}^{M} a_j \varphi(r_j), \tag{3}$$

where r_j represents the radial distance, which is expressed as $r_j = \left|\mathbf{x} - \mathbf{y}_j\right|$; $\varphi(r_j)$ represents the RBF depending only on the distance between $\mathbf{x}$ and $\mathbf{y}_j$; $\mathbf{y}_j$ denotes centers (or source points); $\mathbf{x}$ represents an arbitrary collocation point; a_j represents unknown coefficient to be determined; and M denotes the total number of the collocation points. The MQ RBF can be expressed as $\varphi(r_j) = \sqrt{(r_j\varepsilon)^2 + 1}$. Taking the derivative of the MQ RBF for the Equation (1), the shape parameter, ε, while $r_j = 0$, must be introduced [46] to avoid the singularity.

It is known that the shape parameter can be used to scale the basis function. A small value of ε may flatten the basis function. On the other hand, a large value of ε may generate a steep function. In such a case, the accuracy of the results may depend on the value of the shape parameter. Several methods have been proposed to find the optimal values of the shape parameter. However, determining the optimal shape parameter of MQ function may still be very challenging [32,47].

In this study, we propose a novel collocation meshfree approach, which approximates the numerical solution using the RPBF as follows

$$u(\mathbf{x}) = \sum_{j=1}^{M_O} \sum_{k=1}^{M_N} a_{j,k} r_j^{k+2}, \tag{4}$$

where $r_j = \left|\mathbf{x} - \mathbf{y}_j^s\right|$, $\mathbf{y}_j^s$ is the source point, $\mathbf{x}$ represents the collocation point, $a_{j,k}$ is unknown coefficient to be determined, k represents the order of the radial polynomial, M_N is the number of terms for the radial polynomial and M_O denotes the source point number. When comparing it to the RBFCM, it can be seen that the MQ basis function is replaced by the radial polynomial, which can be expressed as

$$\varphi(r_j) = \sum_{k=1}^{M_N} r_j^{k+2}. \tag{5}$$

To avoid the singularity while discretizing the above RPBF for the governing equation, we adopt the degree of the radial polynomial from original k into $k+2$ for second-order differential equations. For Equation (1), we may obtain the following equation by taking the first derivative of u with respect to x for Equation (4).

$$\frac{\partial u}{\partial x} = \sum_{j=1}^{M_O} \left(\sum_{k=1}^{M_N} a_{j,k} (k+2)(x - x_j^s) r_j^k \right). \tag{6}$$

Taking the first derivative of u with respect to y for Equation (4), we have

$$\frac{\partial u}{\partial y} = \sum_{j=1}^{M_O} \left(\sum_{k=1}^{M_N} a_{j,k} (k+2)(y - y_j^s) r_j^k \right). \tag{7}$$

Similarly, the second derivative of u with respect to x and y for Equations (6) and (7) can also be found.

$$\frac{\partial^2 u}{\partial x^2} = \sum_{j=1}^{M_O}\left(\sum_{k=1}^{M_N} a_{j,k}\left((k+2)r^k + k(k+2)(x - x_j^s)^2 r_j^{k-2}\right)\right), \tag{8}$$

$$\frac{\partial^2 u}{\partial y^2} = \sum_{j=1}^{M_O}\left(\sum_{k=1}^{M_N} a_{j,k}\left((k+2)r^k + k(k+2)(y - y_j^s)^2 r_j^{k-2}\right)\right). \tag{9}$$

Therefore, the two-dimensional Laplacian term can be obtained as follows.

$$\sum_{j=1}^{M_O}\left(\sum_{k=1}^{M_N} a_{j,k}(k+2)^2 r_j^k\right) = 0. \tag{10}$$

We consider the two-dimensional nonhomogeneous modified Helmholtz equation as follows.

$$Du(\mathbf{x}) = f(\mathbf{x}) \text{ in } \Omega, \text{ where } D = \Delta - \lambda^2. \tag{11}$$

The above equation can be discretized using the RPBF as follows.

$$\sum_{j=1}^{M_O}\left(\sum_{k=1}^{M_N} \mathrm{a}_{j,k}(k+2)^2 r_j^k\right) - \lambda^2 \sum_{j=1}^{M_O}\left(\sum_{k=1}^{M_N} \mathrm{a}_{j,k} r_j^{k+2}\right) = f(\mathbf{x}). \tag{12}$$

In the above formulation, a novel meshfree approach with radial polynomial based on the strong form is presented. We collocate M_i inner points and M_b boundary points within the domain and on the boundary, respectively. Considering the boundary data, we may obtain the following system of linear equations

$$\mathbf{Ac} = \mathbf{B}, \tag{13}$$

where $\mathbf{A}$ denotes the square matrix of radial polynomial with the size of $M_r \times M_c$, where $M_r = M_i + M_b$ and $M_c = M_O \times M_N$. $\mathbf{c}$ represents the unknown coefficients, which are $M_c \times 1$ vectors; and $\mathbf{B}$ is the given function from boundary data with the size of $M_r \times 1$. To create a determined system of simultaneous equations, which is $M_r = M_c$, the numbers of source, inner and the boundary points, and the terms of radial polynomial have to be chosen properly. Usually, we may decide the M_c first. The number of boundary points, M_b, can then be found by using $M_c - M_i$. The condition number [48] adopted in this study is defined by

$$\mathrm{Cond}(\mathbf{A}) = \|\mathbf{A}\|\|\mathbf{A}^{-1}\|. \tag{14}$$

Equation (13) can then be rewritten as follows.

$$\begin{bmatrix} \mathbf{A}_\mathrm{I} \\ \mathbf{A}_\mathrm{B} \end{bmatrix}[\mathbf{c}] = \begin{bmatrix} \mathbf{B}_\mathrm{I} \\ \mathbf{B}_\mathrm{B} \end{bmatrix}, \tag{15}$$

where $\mathbf{A}_\mathrm{I}$ is a $M_i \times M_c$ matrix for the inner points; $\mathbf{A}_\mathrm{B}$ represents a $M_b \times M_c$ matrix for the boundary points; $\mathbf{B}_\mathrm{I}$ denotes the function values at the inner points, which are $M_i \times 1$ vectors; and $\mathbf{B}_\mathrm{B}$ denotes the function values at the boundary points with the size of $M_b \times 1$. For examining the accuracy of the proposed approach, we adopt the absolute error and the root mean square error (RMSE) as follows.

$$\text{Absolute error} = \left|\hat{u}(\mathbf{x}_i) - u(\mathbf{x}_i)\right|, \tag{16}$$

$$\mathrm{RMSE} = \sqrt{\frac{1}{M_i}\sum_{i=1}^{M_i}\left(\hat{u}(x_i) - u(x_i)\right)^2}, \tag{17}$$

where $u(\mathbf{x}_i)$ is the exact solution at the inner points, $\hat{u}(\mathbf{x}_i)$ is the numerical solution at the inner points and M_i denotes the inner point number in the domain.

3. Numerical Examples

3.1. Modeling of a Two-Dimensional Laplace Equation

The first example is a two-dimensional Laplacian problem. The governing equation of the Laplacian problem can be expressed as follows.

$$\Delta u(x, y) = 0, (x, y) \in \Omega. \tag{18}$$

The boundary shape is defined as

$$\partial\Omega = \left\{ (x, y) \middle| x = \rho \cos\theta, y = \rho \sin\theta, 0 \le \theta \le 2\pi \right\},\ \rho = 0.5\left|\sec(3\theta)^{\sin(6\theta)}\right|. \tag{19}$$

The exact solution is designated as

$$u(x, y) = e^x \cos y + e^y \sin x. \tag{20}$$

In our proposed meshfree approach, the maximum absolute error (MAE) is adopted for evaluation by

$$\mathrm{MAE} = max\left|\hat{u}(\mathbf{x}_i) - u(\mathbf{x}_i)\right|. \tag{21}$$

In the numerical implementation, M_N is set to be 18. The Dirichlet boundary data are imposed on the boundary adopting the exact solution. Figure 1 depicts the layout of the boundary, source and inner points. In the proposed method, the number of terms for the RPBF, M_N, is the only parameter, which needs to be given for the analysis. To further clarify how to determine the parameter, we conduct a convergence analysis for the M_N. A series of numerical tests have been conducted. The results are presented in Figure 2. Figure 2 demonstrates the MAE versus M_N. It was found that the MAE is always smaller than 10^{-10} for the value of M_N from 15 to 30. The results show that the accuracy is not sensitive to the value of M_N. The most accurate results of the proposed method can be obtained within the order of 10^{-12} while $M_N = 18$. Figure 3 shows the results comparison. The computed solutions agree with the exact solution very well.

To compare our proposed method with the RBFCM using the MQ, we conduct several test cases. Table 1 demonstrates the results comparison between the proposed RPBF and the MQ RBF. Since the MQ RBF needs to decide the shape parameter, we first decide the optimal shape parameter for the MQ RBF. Then, the numerical solutions of the MQ RBF are approximated using the optimal shape parameter. For the proposed approach, we adopt $M_N = 18$ for all the cases based on the results from Figure 2. To further interpret the characteristics of the proposed method, several numerical experiments with different matrix sizes are conducted. Based on the optimal shape parameter and $M_N = 18$ for the proposed RPCM and the MQ RBF, the computed results of numerical experiments are listed in Table 1. The condition numbers with various collocation points are also revealed. It was found that the accuracy of the proposed method is better than the MQ RBF with the same number of collocation points. Additionally, it was also found that the best accuracy of the proposed method can reach up to the order of 10^{-12}. The comparison of the CPU time also demonstrates the efficiency of the proposed method.

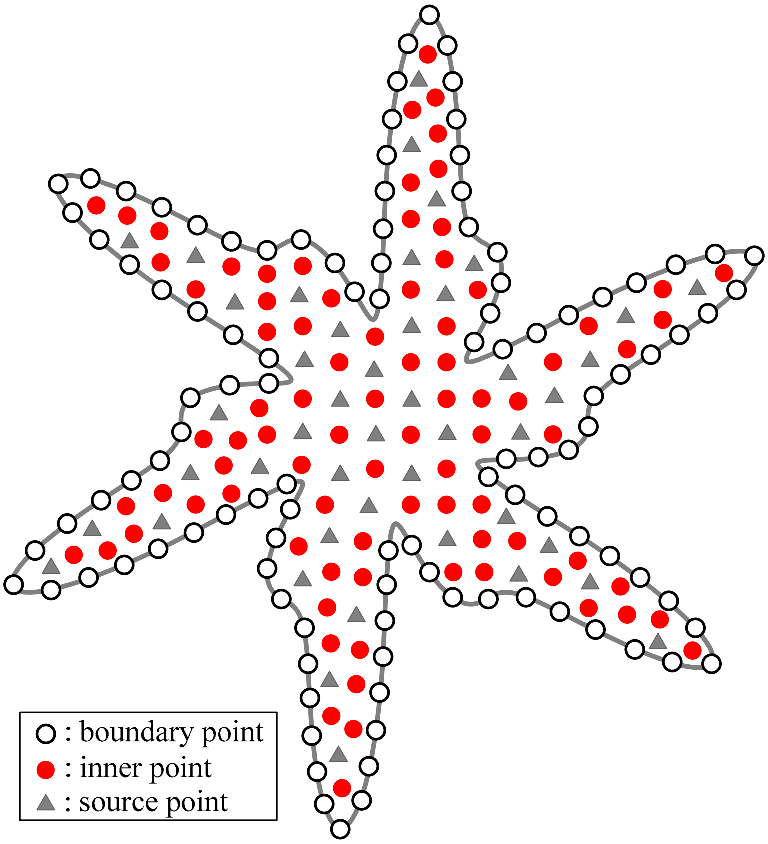

Figure 1. Layout of boundary, source and inner points for example 3.1.

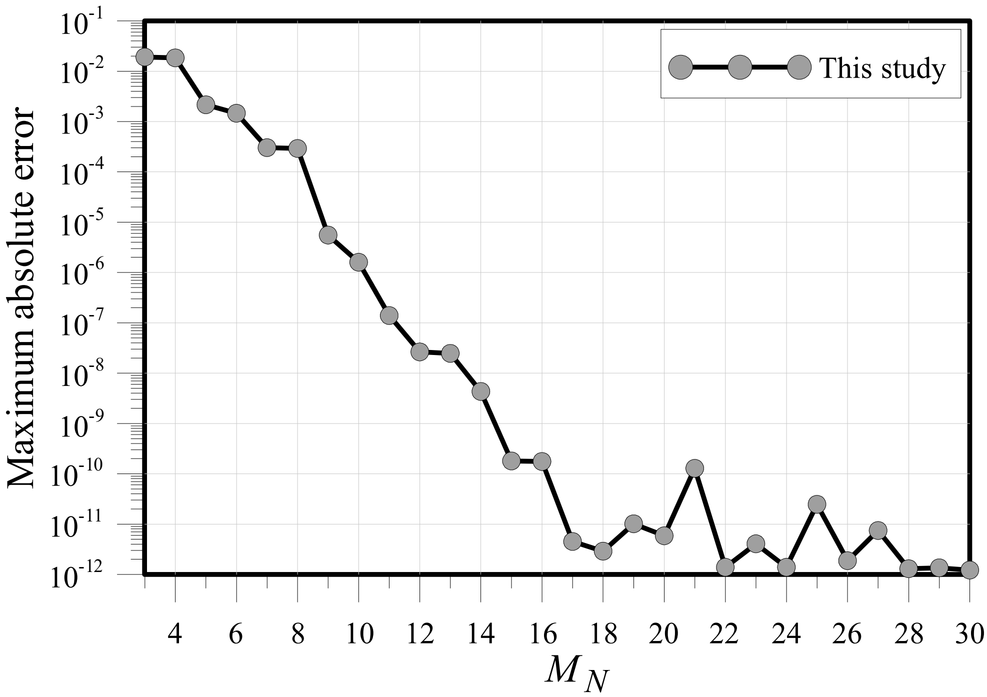

Figure 2. The number of terms of the radial polynomial basis function versus maximum absolute error.

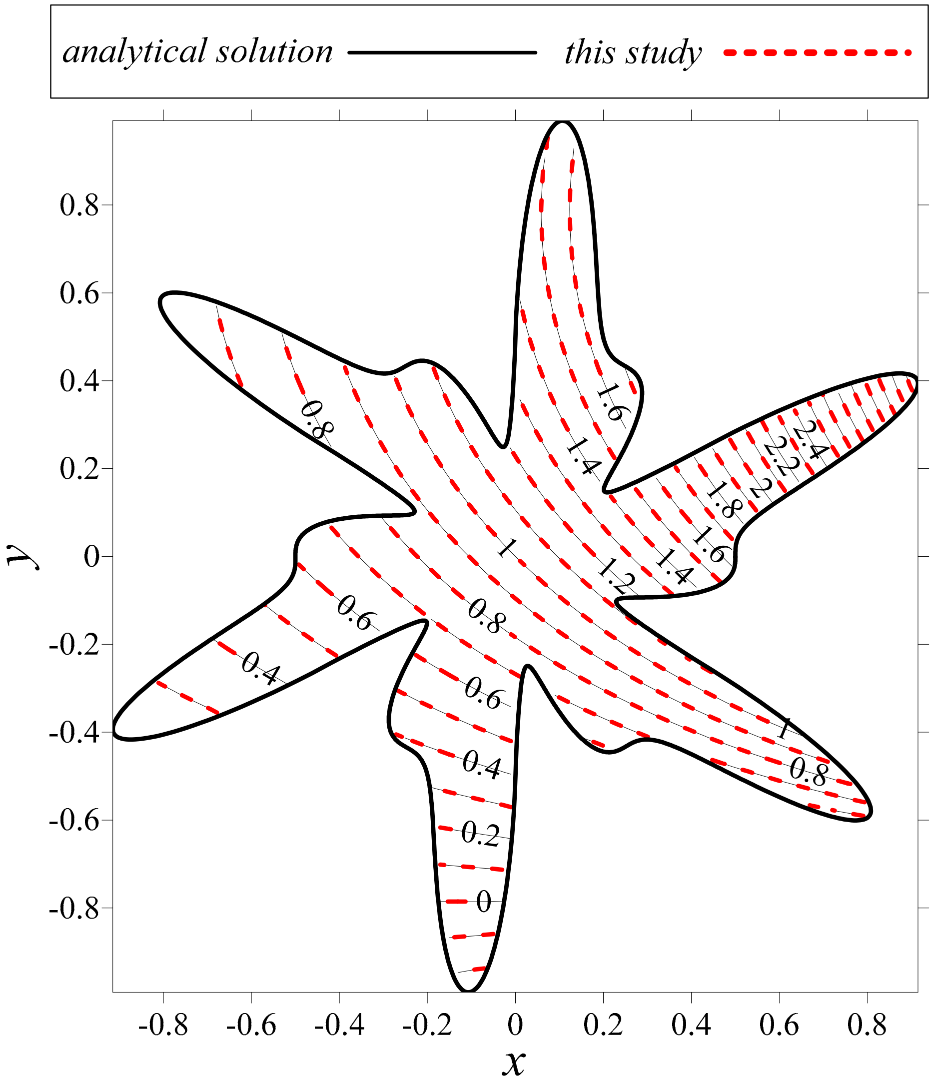

Figure 3. Results comparison between this study and the analytical solution.

Table 1. Results comparison between this study and the multiquadrics radial basis function with the optimal shape parameter.

M_i	M_b	Condition Number	MAE		CPU Time (s)	
		This Study	This Study	MQ RBF	This Study	MQ RBF
471	357	4.26×10^{24}	1.05×10^{-11}	1.17×10^{-5} $(c = 1.8)$	0.79	1.25
812	556	8.08×10^{25}	3.31×10^{-12}	1.04×10^{-5} $(c = 1.4)$	3.78	6.06
1471	1265	9.96×10^{23}	3.44×10^{-11}	1.17×10^{-6} $(c = 1.5)$	12.68	39.58
2486	2176	2.04×10^{25}	3.09×10^{-12}	1.30×10^{-6} $(c = 1.45)$	58.60	188.81
4056	3612	1.12×10^{25}	7.42×10^{-11}	8.31×10^{-7} $(c = 1.1)$	248.43	834.01
5808	5334	4.98×10^{24}	1.01×10^{-10}	1.62×10^{-6} $(c = 1.05)$	730.76	2532.95

3.2. Modeling of a Two-Dimensional Modified Helmholtz Equation

In the second example, we consider the two-dimensional modified Helmholtz equation.

$$(\Delta - \lambda^2)u(x,y) = 0, (x,y) \in \Omega. \tag{22}$$

The boundary shape is defined as

$$\partial\Omega = \left\{(x,y)\middle|x = \rho\cos\theta, y = \rho\sin\theta, 0 \le \theta \le 2\pi\right\}, \text{ where } \rho = 0.5\left|\tan(4\theta)^{\sin(8\theta)}\right|. \tag{23}$$

The exact solution may be found by

$$u(x,y) = e^{(\lambda/2)(x+\sqrt{3}y)}. \tag{24}$$

In this example, M_N is set to be 18 in the numerical implementation. The wave number is $\sqrt{2}$. The Dirichlet boundary data are imposed on the boundary adopting the exact solution. Figure 4 depicts the layout of the collocation points. In this case, we also conduct a convergence analysis for the M_N. It was found that the MAE is always smaller than 10^{-12} for the value of M_N from 17 to 30, as shown in Figure 5. Figure 6 shows the results comparison with the exact solution. It seems that the numerical solutions agree with the exact solution very well.

To compare the proposed method with the MQ RBF, we conduct several numerical experiments. Table 2 demonstrates the results comparison between the proposed method and the MQ RBF. In Table 2, $M_N = 18$ is adopted for the proposed method. Again, it was found that the accuracy of the proposed method is better than the MQ RBF with the same number of collocation points.

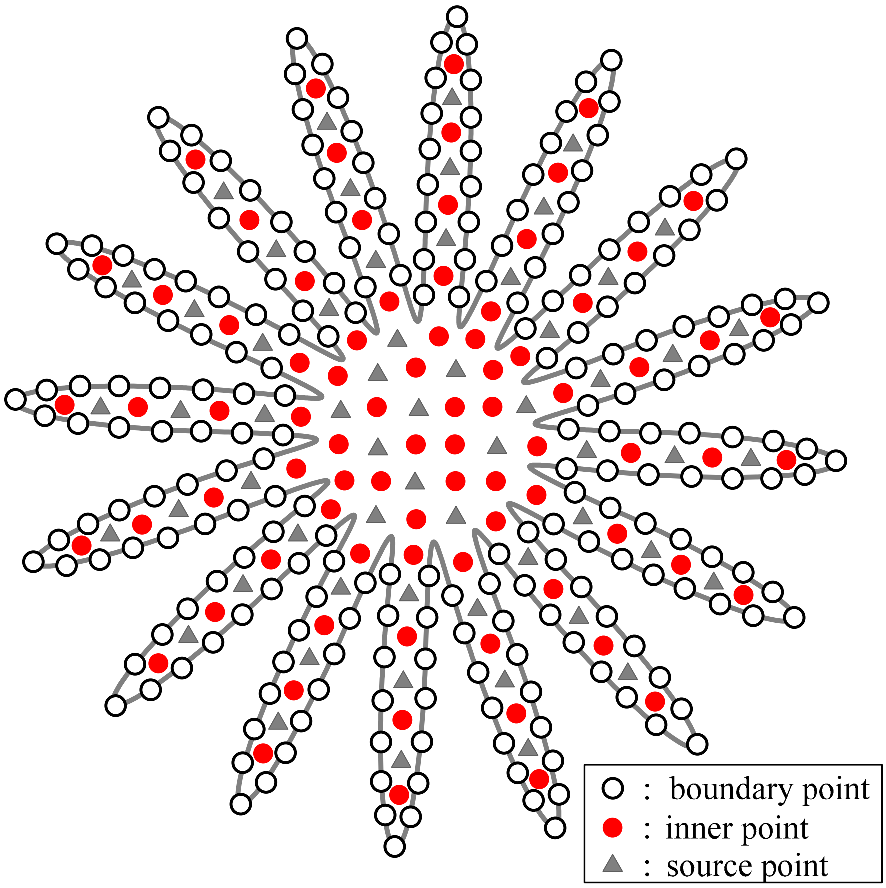

Figure 4. Layout of boundary, source and inner points.

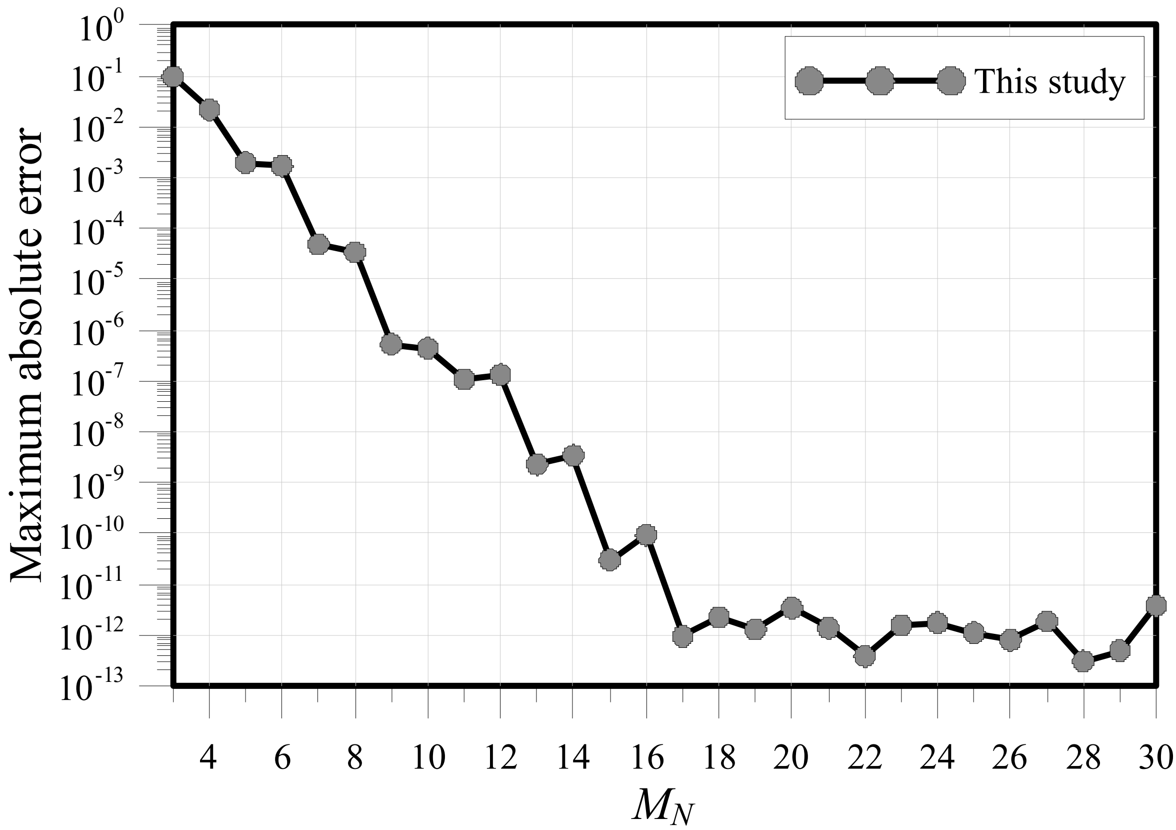

Figure 5. The number of terms of the radial polynomial basis function versus maximum absolute error.

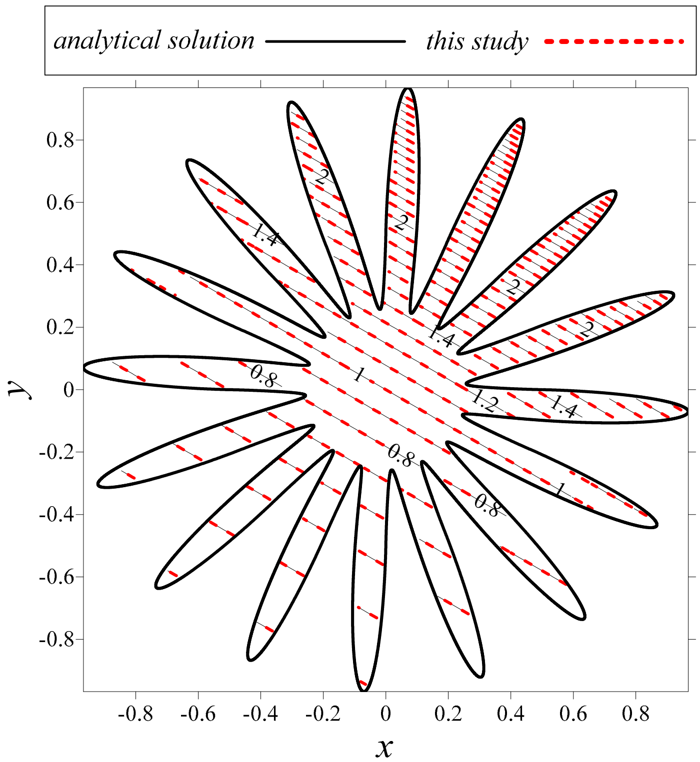

Figure 6. Results comparison between this study and the analytical solution.

Table 2. Results comparison between this study and the multiquadrics radial basis function with the optimal shape parameter.

M_i	M_b	MAE	
		This Study	**MQ RBF**
537	211	5.16×10^{-12}	2.72×10^{-6} ($c = 2.3$)
840	486	6.70×10^{-13}	7.13×10^{-6} ($c = 1.65$)
1579	1192	2.74×10^{-12}	4.71×10^{-5} ($c = 1.95$)
2056	1548	3.32×10^{-12}	1.76×10^{-5} ($c = 1.35$)
4351	3418	3.26×10^{-11}	1.80×10^{-5} ($c = 1.1$)
6224	5234	3.31×10^{-12}	5.43×10^{-6} ($c = 1.4$)

3.3. Modeling of a Two-Dimensional Poisson Equation

The third example is a two-dimensional Poisson problem enclosed by a simply connected region with an irregular domain. The governing equation of the example can be expressed as follows:

$$\Delta u(x,y) = -\pi^2(y\sin(\pi x) + y\cos(\pi y)), (x,y) \in \Omega. \quad (25)$$

The boundary shape is defined as

$$\partial\Omega = \left\{(x,y)\middle|x = \rho\cos\theta, y = \rho\sin\theta, 0 \le \theta \le 2\pi\right\}, \text{ where } \rho = 0.5\left|\sin(4\theta)^{\cos(8\theta)}\right|. \quad (26)$$

The exact solution is designated as

$$u(x,y) = y\sin(\pi x) + x\cos(\pi y). \quad (27)$$

In this example, M_N is set to be 18. The Dirichlet boundary data are imposed on the boundary adopting the exact solution. Figure 7 depicts the layout of the boundary, source and inner points. Figure 8 shows the number of terms of the RPBF versus MAE. We can observe that the MAE is always smaller than 10^{-11} for values of M_N from 17 to 30, as shown in Figure 8. Figure 9 shows the MAE versus the collocation point number. It can be found that the promising numerical solutions can be achieved when the boundary point number is greater than 430. On the other hand, Figure 9 also depicts the MAE versus the inner point number. The accurate results with the accuracy within the order of 10^{-11} are obtained when the inner point number is greater than 385. The results from the number of the boundary and inner points show that highly accurate results may be approximated while the numbers of the boundary and inner points are greater than 430 and 385, respectively. Figure 10 shows the results comparison between this study and the exact solution. The numerical solutions agree with the exact solution very well.

The polyharmonic splines (PS) usually refer to the polyharmonic RBF, which is often used with the natural logarithm to avoid singularity. Different from the TPS-RBF approximated the solution using a fixed degree of the polyharmonic RBF, the proposed RPBF may include any degree of the radial polynomial. Another example has been conducted to compare the proposed method with those obtained by Chen et al., 2010 [49].

Again, $M_N = 18$ is adopted in this specific example. Table 3 demonstrates the results comparison between the proposed method and the PS RBF [49]. It was found that the accuracy of the proposed method is better than that of PS RBF with the same number of collocation points. Additionally, it was also found that the best accuracy of the proposed method can reach up to the order of 10^{-12}.

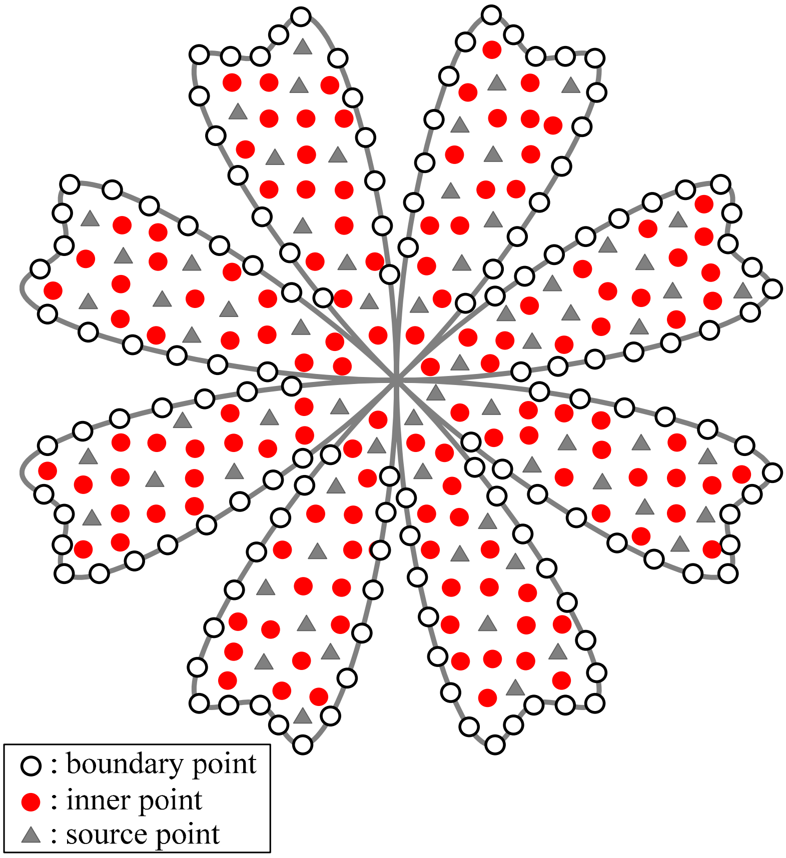

Figure 7. Layout of the boundary, source and inner points.

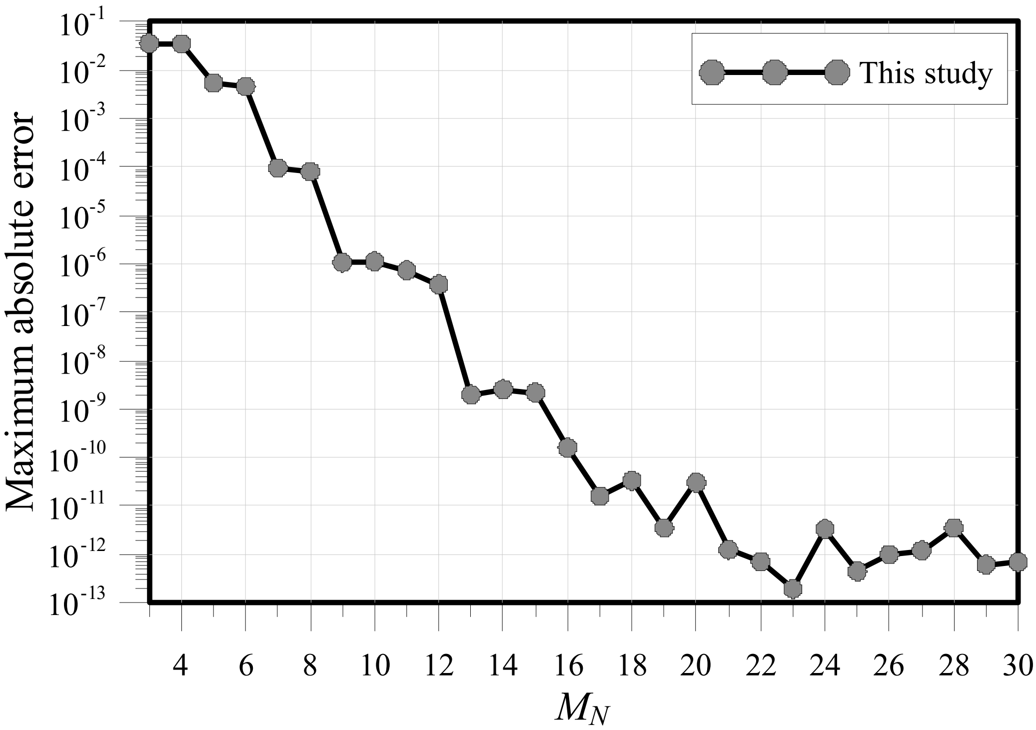

Figure 8. The number of terms of the radial polynomial basis function versus maximum absolute error.

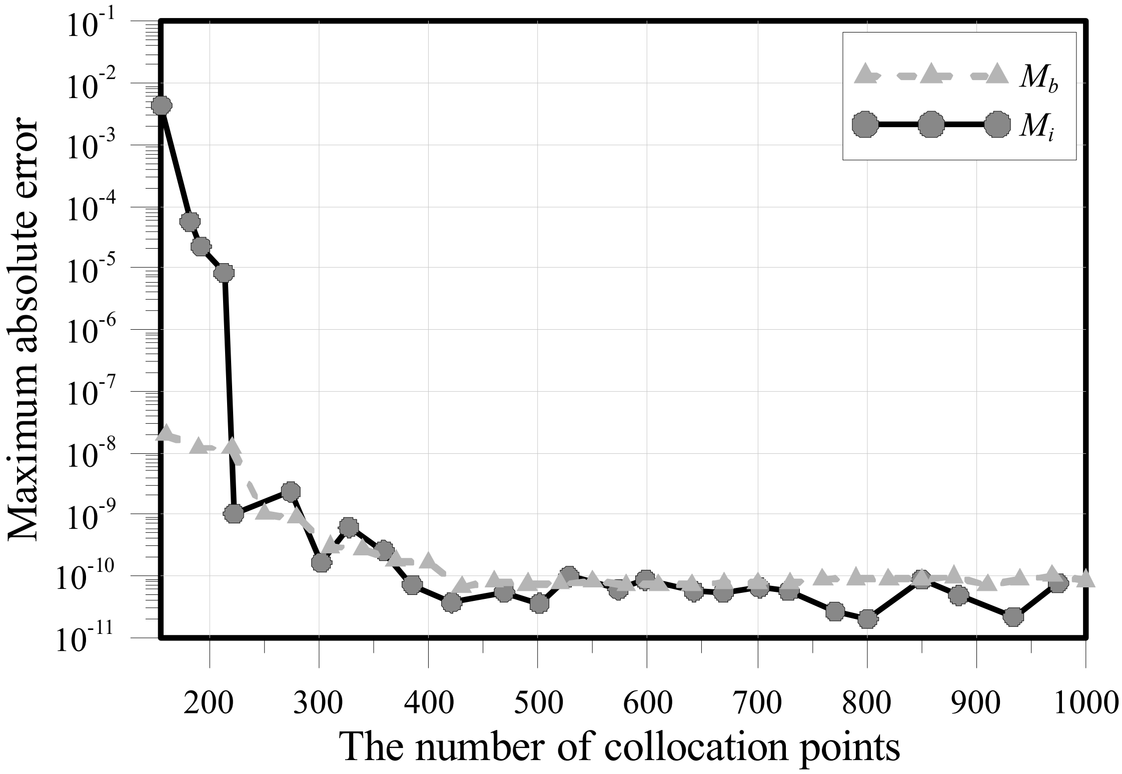

Figure 9. The boundary point number versus the maximum absolute error.

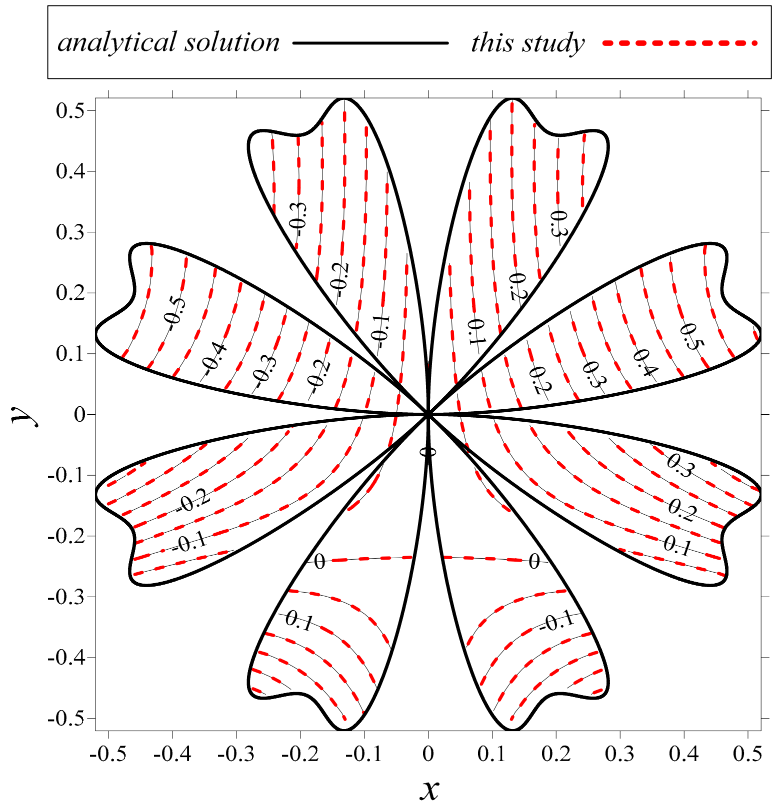

Figure 10. Results comparison between this study and the analytical solution.

Table 3. Results comparison between this study and the PS RBF.

Collocation Point Number	RMSE	
	This Study (M_N=18)	PS RBF[49]
$M_b = 80, M_i = 208$	6.99×10^{-7}	1.87×10^{-4}
$M_b = 120, M_i = 284$	7.75×10^{-8}	5.39×10^{-5}
$M_b = 160, M_i = 406$	4.39×10^{-8}	1.92×10^{-5}
$M_b = 921, M_i = 645$	3.89×10^{-12}	NA

3.4. Modeling of a Two-Dimensional Nonhomogeneous Modified Helmholtz Equation

The fourth example is the modeling of a two-dimensional nonhomogeneous modified Helmholtz equation enclosed by a simply connected region in an irregular domain, as shown in Figure 11. The governing equation of the example can be expressed as follows:

$$(\Delta - \lambda^2)u(x, y) = (1 - \lambda^2)(\sin hx + \cos hy), (x, y) \in \Omega. \tag{28}$$

The boundary shape is defined as

$$\partial\Omega = \left\{(x, y)\middle|x = \rho\cos\theta, y = \rho\sin\theta, 0 \le \theta \le 2\pi\right\}, \text{ where } \rho = 0.5\left|\sin(2\theta)^{\cos(4\theta)}\right|. \tag{29}$$

The exact solution may be found as

$$u(x, y) = \sin hx + \cos hy. \tag{30}$$

According to Figure 12, M_N is set to be 18 again. The Dirichlet boundary data are imposed on the boundary adopting the exact solution. Figure 11 depicts the layout of the boundary, source and inner points. Figure 13 shows the results comparison with the exact solution. It was found that the numerical solutions agree with the exact solution very well. The accuracy of the solutions may be affected by the wave number severely. To examine the influence of λ^2 on the accuracy, we conduct several numerical experiments. The results of the numerical cases are presented in Table 4. From Table 4, it is demonstrated that our proposed method may obtain accurate results for the values of λ^2 ranging from 16 to 10,000.

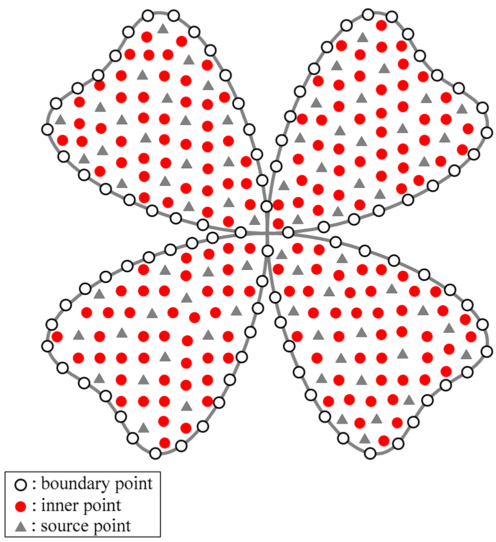

Figure 11. Layout of the boundary, source and inner points.

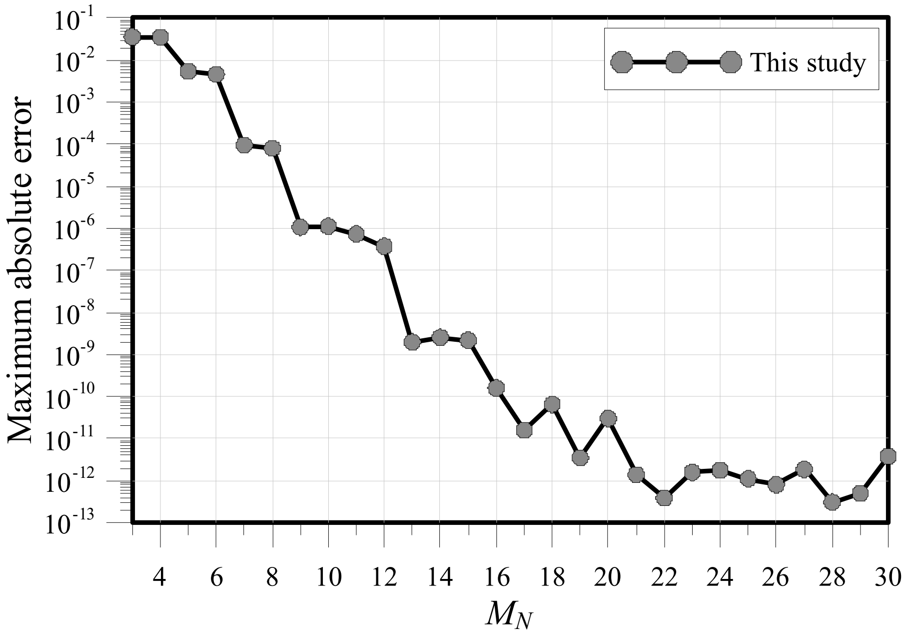

Figure 12. The number of terms of the radial polynomial basis function versus maximum absolute error.

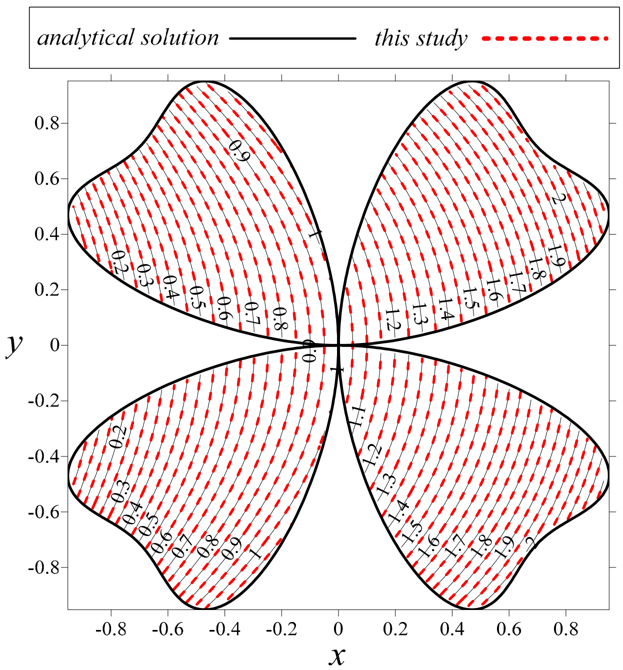

Figure 13. Results comparison between this study and the analytical solution.

Table 4. Maximum absolute error for different λ^2.

λ^2	MAE
16	2.67×10^{-12}
25	4.23×10^{-13}
36	7.36×10^{-12}
100	1.64×10^{-12}
2000	3.29×10^{-13}
4000	1.39×10^{-13}
6000	5.24×10^{-13}
8000	8.06×10^{-13}
10,000	3.82×10^{-13}

3.5. Modeling of a Nonhomogeneous Modified Helmholtz Equation in a Doubly Connected Region

The fifth example is a nonhomogeneous modified Helmholtz problem in a doubly connected domain. The governing equation can be expressed as follows.

$$(\Delta - 900)u(x, y) = -899(e^x + e^y), (x, y) \in \Omega. \tag{31}$$

The doubly connected domain is bounded by a star-like outer boundary ($\partial\Omega_1$) and a peanut-like inner boundary ($\partial\Omega_2$). The irregular domain in two dimensions is described by

$$\partial\Omega_1 = \left\{(x_1, y_1)\middle| x_1 = \rho_1 \cos\theta_1, y_1 = \rho_1 \sin\theta_1, 0 \le \theta_1 \le 2\pi\right\},\ \rho_1 = 1 + \cos^2(4\theta_1), \tag{32}$$

$$\begin{gathered} \partial\Omega_2 = \left\{(x_2, y_2)\middle| x_2 = \rho_2 \cos\theta_2, y_2 = \rho_2 \sin\theta_2, 0 \le \theta_2 \le 2\pi\right\}, \\ \rho_2 = 0.5\sqrt{\cos(2\theta_2) + \sqrt{1.1 - (\sin(2\theta_2))^2}}. \end{gathered} \tag{33}$$

The analytical solution may be found as

$$u(x, y) = e^x + e^y. \tag{34}$$

In the numerical implementation, M_N, is set to be 18. The Dirichlet boundary data are imposed on the boundary adopting the exact solution. Figure 14 depicts the layout of collocation points. Figure 15 shows the results comparison with the exact solution. The numerical solutions agree with the exact solution very well.

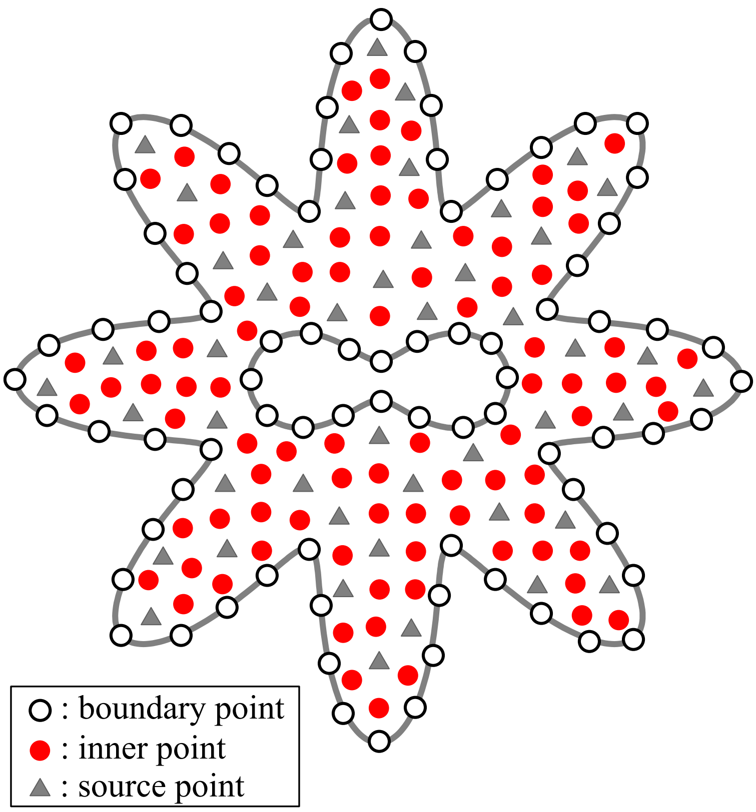

Figure 14. Layout of boundary, source and inner points.

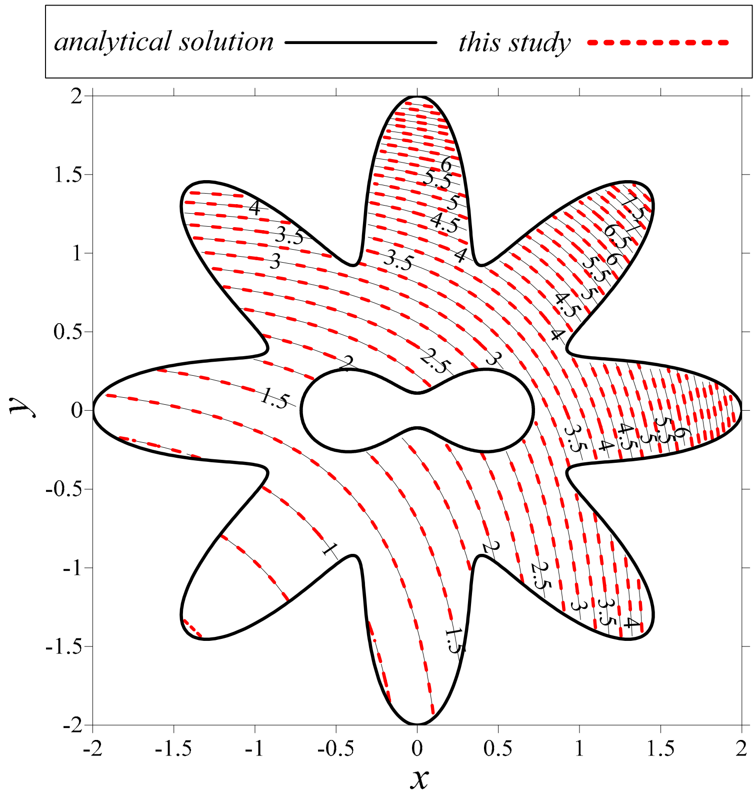

Figure 15. Results comparison between this study and the analytical solution.

3.6. Modeling of the General Elliptic Partial Differential Equation

In the last example, a more general elliptic partial differential equation enclosed by an amoeba-like domain boundary is considered. The governing equation to be solved is expressed as follows.

$$\Delta u + (y^2 \sin x)\frac{\partial u}{\partial x} + (xe^y)\frac{\partial u}{\partial y} + (\sin x + \cos y)u = d(x,y), (x,y), \in \Omega. \tag{35}$$

The exact solution may be designated as follows

$$u(x,y) = y\sin(\pi x) + x\cos(\pi y). \tag{36}$$

The unknown function, $d(x,y)$, can then be derived from the exact solution as follows.

$$\begin{aligned} d(x,y) = \quad & (y\sin(\pi x) + x\cos(\pi y))\left(-\pi^2 + (\sin x + \cos y)\right) + (y^2 \sin x)(\pi y\cos(\pi x) + \cos(\pi y)) + \\ & xe^y(\sin(\pi x) - \pi x\sin(\pi y)) \end{aligned} \tag{37}$$

The amoeba-like boundary is defined as follows.

$$\partial\Omega = \left\{(x,y)\middle| x = \rho\cos\theta, y = \rho\sin\theta, 0 \le \theta \le 2\pi\right\}, \rho = 0.5\left(e^{(\sin\theta\sin 2\theta)2} + e^{(\cos\theta\cos 2\theta)2}\right). \tag{38}$$

In this case, $M_N = 18$. The Dirichlet boundary data are imposed on the boundary using the exact solution. Figure 16 depicts the layout of the source, boundary and inner points. Figure 17 shows the MAE versus the boundary point number. It is apparent that the promising numerical solutions can be achieved when the boundary point number is greater than 1800. On the other hand, Figure 18 depicts the MAE versus the inner point number. The results with the accuracy within the order of 10^{-11} are obtained when the inner point number is greater than 300. Figure 19 displays the results comparison between this study and the exact solution. The numerical solutions agree with the exact solution very well.

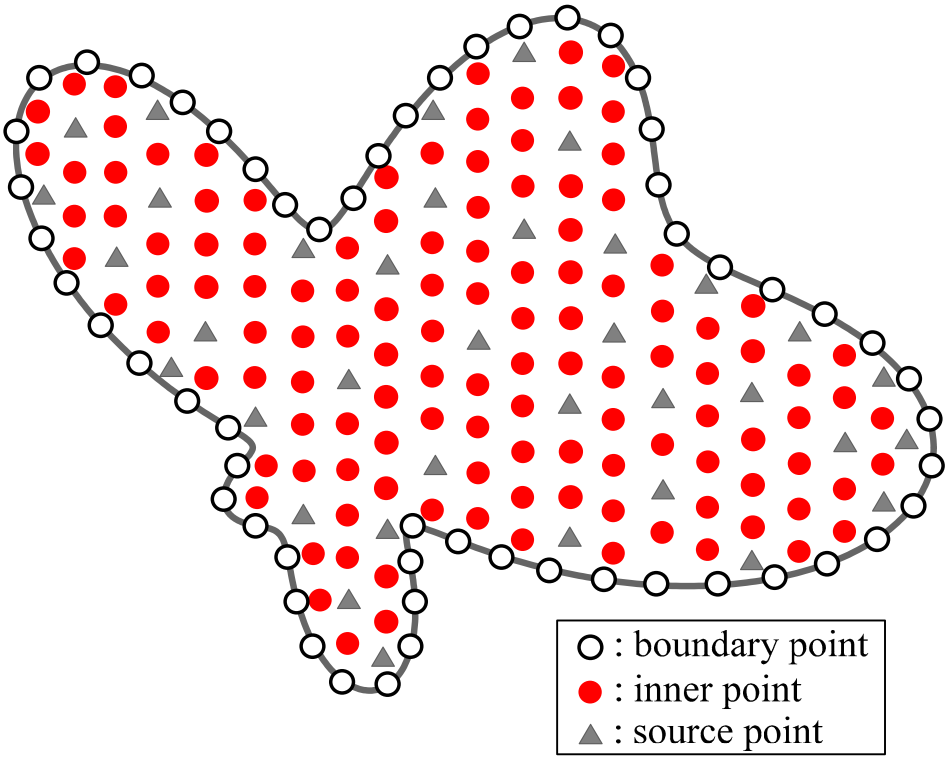

Figure 16. Layout of boundary, source and inner points.

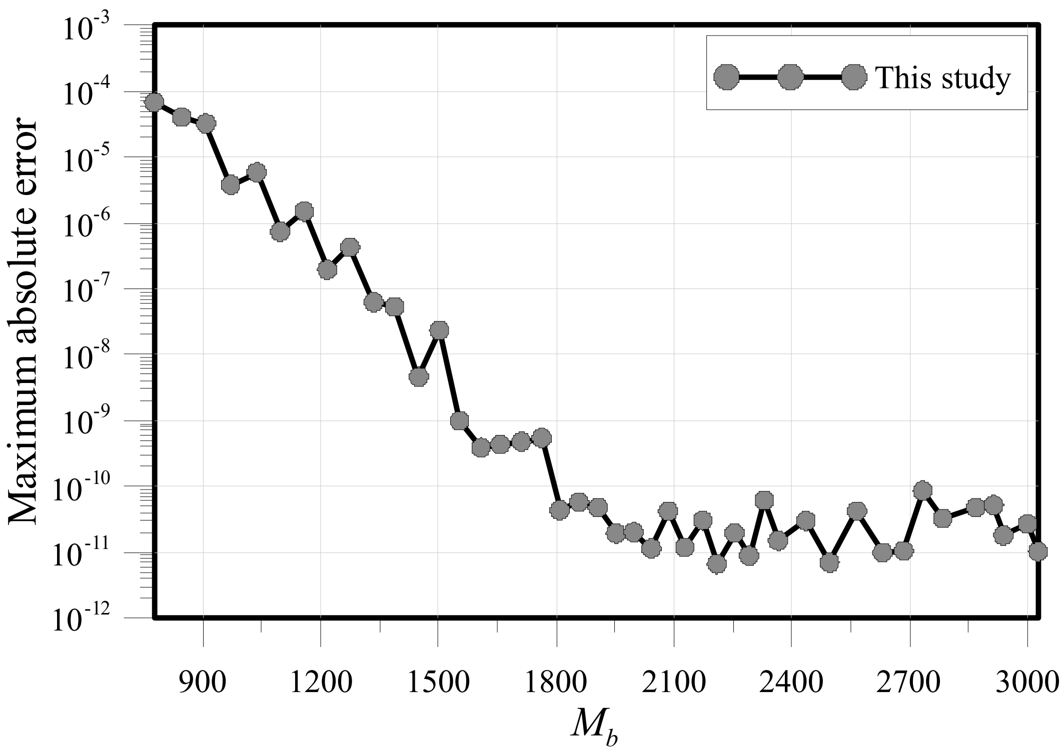

Figure 17. The number of boundary points versus the maximum absolute error.

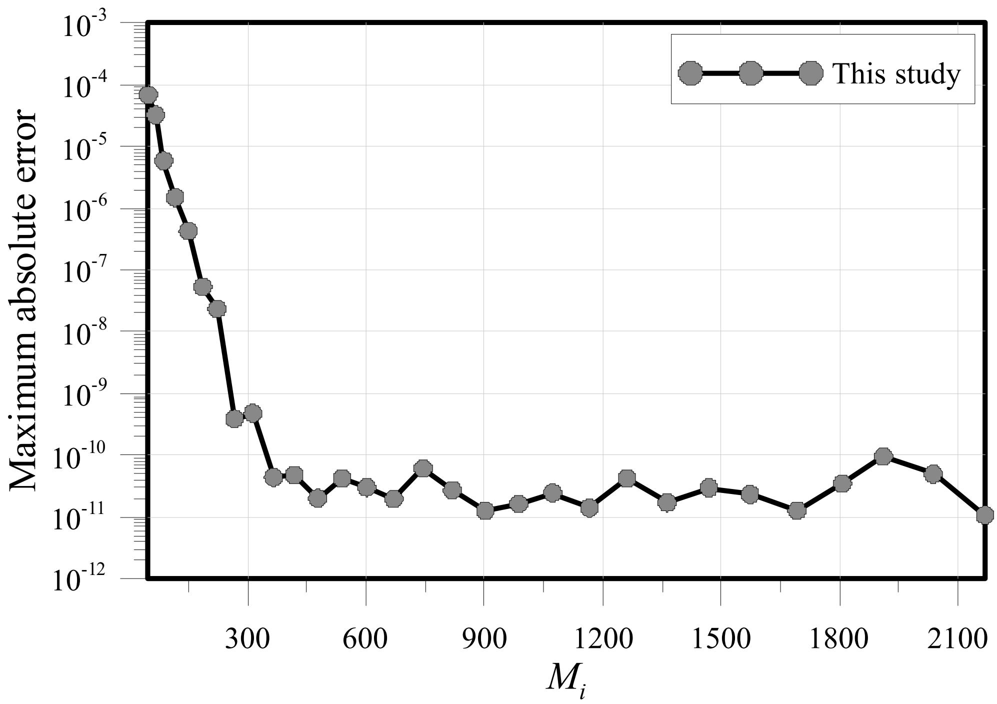

Figure 18. The number of inner points versus the maximum absolute error.

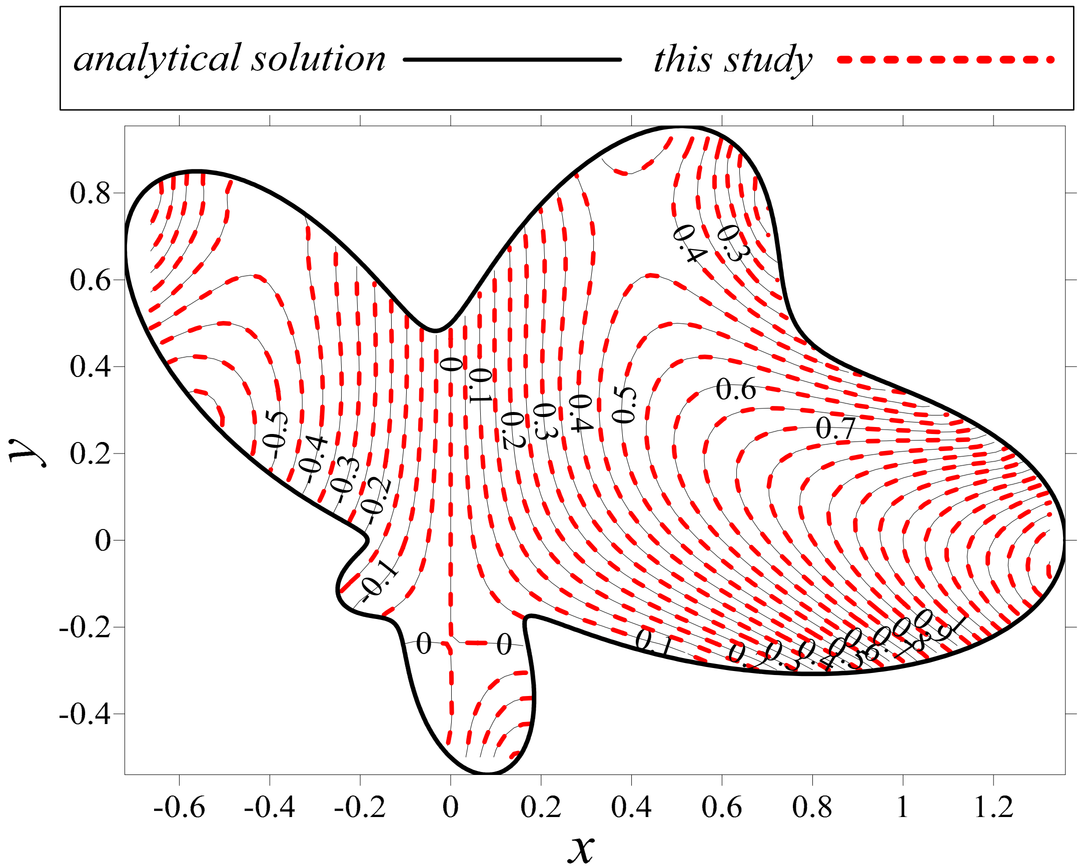

Figure 19. Results comparison between this study and the analytical solution.

4. Discussion

This paper presents a novel, collocation meshfree approach with the RPBF capable of solving two-dimensional, nonhomogeneous partial differential equations. The novel conception of the proposed approach is based on the radial polynomial. The advantages of the proposed approach are as follows.

To avoid the singularity in the derivation of the MQ RBF for the governing equation, the shape parameter must be used in the RBFCM. The issue for finding the proper value of the shape parameter is very challenging. To overcome the issue, we propose the RPBF as the basis function. Due to the non-singular characteristics in the RPBF, it was found that the derivation of the RPBF in the discretization of the governing equation is also a non-singular function. As a result, we do not require the shape parameter in the proposed approach.

The proposed RPBF is the sum of the polyharmonic splines. The polyharmonic splines usually refer to the polyharmonic RBF which is often used with the natural logarithm to avoid singularity. Differently from how the TPS-RBF approximates the solution using a fixed degree of the polyharmonic RBF, the proposed RPBF may include any degree of the radial polynomial. Accordingly, the proposed method may be more general and can obtain highly accurate solutions with the increase of radial polynomial terms. The comparison results between the proposed RPBF and the PS RBF demonstrate that the accuracy of the proposed method is better than the PS RBF with the same number of collocation points. Additionally, it was also found that the best accuracy of the proposed method can reach up to the order of 10^{-12}.

We addressed the convergence properties of the proposed method with the terms of the RPBF, the number of boundary points and the number of inner points. Numerical experiments were also carried out. It was found that the maximum absolute error may reach up to 10^{-11} with the terms of the RPBF greater than 18. Additionally, highly accurate solutions may be obtained if the numbers of boundary points and inner points are greater than 430 and 385, respectively. The convergence analysis depicts that the terms of the RPBF are not very sensitive to the accuracy if M_N is greater than 18.

We demonstrate the proposed approach may be used to solve problems enclosed by a doubly connected domain. We also validate the accuracy of the proposed approach for solving the nonhomogeneous modified Helmholtz equation. It was found that very accurate results may be obtained, in which the MAE is within the order of 10^{-12}, even though the high wave number is considered for the modified Helmholtz equation. Additionally, results show that the proposed approach may obtain more accurate results than those from the RBFCM using the MQ RBF.

5. Conclusions

In this study, we propose a novel collocation meshfree approach for solving nonhomogeneous PDEs. The proposed approach is verified, and numerical examples are also carried out. We may summarize the following findings.

1. In this study, the meshfree approach using RPBF as the basis function is proposed. We resolve a major issue in the RBFCM using the MQ function for finding a satisfactory value for the shape parameter.
2. The proposed method may obtain highly accurate numerical solutions with the use of higher order radial polynomial terms. Numerical examples show that the proposed RPBF is much more accurate than the MQ RBF, even when the optimal shape parameter for the MQ RBF is adopted. Additionally, the comparison results between the proposed RPBF and the PS RBF demonstrate that the accuracy of the proposed method is better than the PS RBF with the same number of collocation points.
3. In this paper, a novel, meshfree approach using the RPBF is first presented. We conduct a pioneering work for solving the nonhomogeneous PDEs bounded by simply and doubly connected domains. The proposed novel method provides a promising solution in which the advantages of the conventional RBFCM are still remained, such as the domain collocation only.

Moreover, the ease of use for solving nonhomogeneous PDEs is revealed, and the tedious procedure to determine the shape parameter is no longer required.

Author Contributions: Conceptualization, C.-Y.K.; data curation, C.-Y.L.; methodology, C.-Y.K. and J.-E.X.; calidation, J.-E.X.; writing—original manuscript, C.-Y.K.; writing—review and editing, C.-Y.K. and J.-E.X. All authors have read and agreed to the published version of the manuscript.

Funding: This research was funded by the Ministry of Science and Technology of R.O.C. (grant number MOST 108-2621-M-019-008).

Acknowledgments: The authors appreciate the editor and the referees for invaluable comments that have enhanced the quality of the paper.

Conflicts of Interest: The authors declare no conflict of interest.

References

1. Lin, Y.; Gao, X.; Xiao, M.Q. A high-order finite difference method for 1D nonhomogeneous heat equations. *Numer. Meth. Part D* **2009**, *25*, 327–346. [CrossRef]
2. Park, Y.S.; Ang, W.T. A complex variable boundary element method for an elliptic partial differential equation with variable coefficients. *Commun. Numer. Meth. Eng.* **2000**, *16*, 697–703. [CrossRef]
3. Fix, G.J.; Gunzburger, M.D.; Peterson, J.S. On finite element approximations of problems having inhomogeneous essential boundary conditions. *Comput. Math. Appl.* **1983**, *9*, 687–700. [CrossRef]
4. Song, R.; Chen, W. An investigation on the regularized meshless method for irregular domain problems. *CMES Comp. Model. Eng.* **2009**, *42*, 59–70.
5. Lin, J.; Chen, C.S.; Liu, C.S. Fast solution of three-dimensional modified Helmholtz equations by the method of fundamental solutions. *Commun. Comput. Phy.* **2016**, *20*, 512–533. [CrossRef]
6. Kuo, L.H.; Gu, M.H.; Young, D.L.; Lin, C.Y. Domain type kernel-based meshless methods for solving wave equations. *CMC Comput. Mater. Contin.* **2013**, *33*, 213–228.
7. Bourantas, G.C.; Skouras, E.D.; Loukopoulos, V.C.; Nikiforidisa, G.C. An accurate, stable and efficient domain-type meshless method for the solution of MHD flow problems. *J. Comput. Phys.* **2009**, *228*, 8135–8160. [CrossRef]
8. Tang, Y.Z.; Li, X.L. Numerical analysis of the meshless element-free Galerkin method for hyperbolic initial-boundary value problems. *Appl. Math.* **2017**, *62*, 477–492. [CrossRef]
9. Sun, F.X.; Liu, C.; Cheng, Y.M. An improved interpolating element-free Galerkin method based on nonsingular weight functions. *Math. Probl. Eng.* **2014**, *2014*, 323945. [CrossRef]
10. Mirzaei, D.; Schaback, R. Direct meshless local Petrov–Galerkin (DMLPG) method: A generalized MLS approximation. *Appl. Numer. Math.* **2013**, *68*, 73–82. [CrossRef]
11. Mirzaei, D.; Hasanpour, K. Direct meshless local Petrov–Galerkin method for elastodynamic analysis. *Acta Mech.* **2016**, *227*, 619–632. [CrossRef]
12. Zhang, H.Q.; Chen, Y.; Guo, C.X.; Fu, Z.H. Application of radial basis function method for solving nonlinear integral equations. *J. Appl. Math.* **2014**, *2014*, 381908. [CrossRef]
13. Seydaoglu, M. A meshless method for Burgers' equation using multiquadric radial basis functions with a Lie-group integrator. *Mathematics* **2019**, *7*, 113. [CrossRef]
14. Cao, Y.; Dong, J.L.; Yao, L.Q. A modification of the moving least-squares approximation in the element-free Galerkin method. *J. Appl. Math.* **2014**, *2014*, 528082. [CrossRef]
15. Assari, P.; Adibi, H.; Dehghan, M. A meshless method based on the moving least squares (MLS) approximation for the numerical solution of two-dimensional nonlinear integral equations of the second kind on non-rectangular domains. *Numer. Algorithms* **2014**, *67*, 423–455. [CrossRef]
16. Fan, C.M.; Li, P.W. Generalized finite difference method for solving two-dimensional Burgers' equations. *Procedia Eng.* **2014**, *79*, 55–60. [CrossRef]
17. Fan, C.M.; Li, P.W.; Yeih, W.C. Generalized finite difference method for solving two-dimensional inverse Cauchy problems. *Inverse Probl. Sci. Eng.* **2015**, *23*, 737–759. [CrossRef]
18. Gu, Y.; Qu, W.Z.; Chen, W.; Song, L.; Zhang, C.Z. The generalized finite difference method for long-time dynamic modeling of three-dimensional coupled thermoelasticity problems. *J. Comput. Phys.* **2019**, *384*, 42–59. [CrossRef]

19. Fornberg, B.; Larsson, E.; Flyer, N. Stable computations with Gaussian radial basis functions. *SIAM. J. Sci. Comput.* **2011**, *33*, 869–892. [CrossRef]
20. Hardy, R.L. Multiquadric equations of topography and other irregular surfaces. *J. Geophys. Res.* **1971**, *76*, 1905–1915. [CrossRef]
21. Faul, A.C.; Powell, M.J.D. Proof of convergence of an iterative technique for thin plate spline interpolation in two dimensions. *Adv. Comput. Math.* **1999**, *11*, 183–192. [CrossRef]
22. Powell, M.J.D. The uniform convergence of thin plate spline interpolation in two dimensions. *Numer. Math.* **1994**, *68*, 107–128. [CrossRef]
23. Assari, P.; Dehghan, M. Application of thin plate splines for solving a class of boundary integral equations arisen from Laplace's equations with nonlinear boundary conditions. *Int. J. Comput. Math.* **2019**, *96*, 170–198. [CrossRef]
24. Bouhamidi, A.; Jbilou, K. Meshless thin plate spline methods for the modified Helmholtz equation. *Comput. Methods Appl. Mech. Engrgy* **2008**, *197*, 3733–3741. [CrossRef]
25. Chen, W.; Tanaka, M. A meshless, integration-free, and boundary-only RBF technique. *Comput. Math. Appl.* **2002**, *43*, 379–391. [CrossRef]
26. Kołodziej, J.A.; Grabski, J.K. Application of the method of fundamental solutions and the radial basis functions for viscous laminar flow in wavy channel. *Eng. Anal. Bound. Elem.* **2015**, *57*, 58–65. [CrossRef]
27. Ben-Ahmed, E.; Sadik, M.; Wakrim, M. Radial basis function partition of unity method for modelling water flow in porous media. *Comput. Math. Appl.* **2018**, *75*, 2925–2941. [CrossRef]
28. Sarler, B. A radial basis function collocation approach in computational fluid dynamics. *CMES Comp. Model. Eng.* **2005**, *7*, 185–193.
29. Li, Y.; Hon, Y.C. Finite integration method with radial basis function for solving stiff problems. *Eng. Anal. Bound. Elem.* **2017**, *82*, 32–42. [CrossRef]
30. Liu, C.S.; Chang, C.W. An energy regularization of the MQ-RBF method for solving the Cauchy problems of diffusion-convection-reaction equations. *Commun. Nonlinear Sci.* **2019**, *67*, 375–390. [CrossRef]
31. Wang, J.G.; Liu, G.R. On the optimal shape parameters of radial basis functions used for 2-D meshless methods. *Comput. Method Appl. Mech. Eng.* **2002**, *191*, 2611–2630. [CrossRef]
32. Fasshauer, G.E.; Zhang, J.G. On choosing "optimal" shape parameters for RBF approximation. *Numer. Algorithms* **2007**, *45*, 345–368. [CrossRef]
33. Rocha, H. On the selection of the most adequate radial basis function. *Appl. Math. Model.* **2009**, *33*, 1573–1583. [CrossRef]
34. Roque, C.M.C.; Ferreira, A.J.M. Numerical experiments on optimal shape parameters for radial basis functions. *Numer. Meth. Part. D* **2010**, *26*, 675–689. [CrossRef]
35. Afiatdoust, F.; Esmaeilbeigi, M. Optimal variable shape parameters using genetic algorithm for radial basis function approximation. *Ain. Shams Eng. J.* **2015**, *6*, 639–647. [CrossRef]
36. Biazar, J.; Hosami, M. An interval for the shape parameter in radial basis function approximation. *Appl. Math. Comput.* **2017**, *315*, 131–149. [CrossRef]
37. Chen, W.; Hong, Y.X.; Lin, J. The sample solution approach for determination of the optimal shape parameter in the Multiquadric function of the Kansa method. *Comput. Math. Appl.* **2018**, *75*, 2942–2954. [CrossRef]
38. Fallah, A.; Jabbari, E.; Babaee, R. Development of the Kansa method for solving seepage problems using a new algorithm for the shape parameter optimization. *Comput. Math. Appl.* **2019**, *77*, 815–829. [CrossRef]
39. Chen, C.S.; Lee, S.W.; Huang, C.S. Derivation of particular solutions using Chebyshev polynomial based functions. *Int. J. Comp. Meth.* **2011**, *4*, 15–32. [CrossRef]
40. Tsai, C.C. Particular solutions of Chebyshev polynomials for polyharmonic and poly-Helmholtz equations. *CMES-Comp. Model. Eng.* **2008**, *27*, 151–162.
41. Dangal, T.; Chen, C.S.; Lin, J. Polynomial particular solutions for solving elliptic partial differential equations. *Comput. Math. Appl.* **2017**, *73*, 60–70. [CrossRef]
42. Lin, J.; Chen, C.S.; Wang, F.J.; Dangal, T. A new backward node interpolation method using polynomial basis functions for plane bending vibrations. *Appl. Math. Model.* **2017**, *49*, 452–469. [CrossRef]
43. Ahmed, S.G. A collocation method using new combined radial basis functions of thin plate and multiquadraic types plate. *Eng. Anal. Bound. Elem.* **2006**, *30*, 697–701. [CrossRef]
44. Xiang, S.; Bi, Z.Y.; Jiang, S.X.; Jin, Y.X.; Yang, M.S. Thin plate spline radial basis function for the free vibration analysis of laminated composite shells. *Compos. Struct.* **2011**, *93*, 611–615. [CrossRef]

45. Muleshkov, A.S.; Golberg, M.A.; Chen, C.S. Particular solutions of Helmholtz-type operators using higher order polyhrmonic splines. *Comput. Mech.* **1999**, *23*, 411–419. [CrossRef]
46. Kansa, E.J. Multiquadrics—A scattered data approximation scheme with applications to computational fluid-dynamics—II solutions to parabolic, hyperbolic and elliptic partial differential equations. *Comput. Math. Appl.* **1990**, *19*, 147–161. [CrossRef]
47. Liu, C.S.; Liu, D.J. Optimal shape parameter in the MQ-RBF by minimizing an energy gap functional. *Appl. Math. Lett.* **2018**, *86*, 157–165. [CrossRef]
48. Liu, C.S. Improving the ill-conditioning of the method of fundamental solutions for 2D Laplace equation. *CMES-Comp. Model. Eng.* **2009**, *851*, 1–17.
49. Chen, C.S.; Fan, C.M.; Wen, P.H. The method of particular solutions for solving certain partial differential equations. *Numer. Meth. Part. D* **2012**, *28*, 506–522. [CrossRef]